Spin-Label Studies on the Aqueous Regions of Phospholipid Multilayers†

Alec D. Keith,* Wallace Snipes,* and Dennis Chapman‡

ABSTRACT: Water-soluble spin labels were used to study dimyristoyllecithin (DML) phospholipid multilayers. Previous studies report that there is a "bound" water region associated with dimyristoyllecithin containing about 10 molecules of water per phospholipid, a "trapped" water region located between the lamellae containing approximately 11 molecules per phospholipid, and a "free" water region external to the lamellae. The results of this investigation show that certain water-soluble spin-label molecules have their motional properties differentially modified by these three water environments. Furthermore, the labels also reveal the onset of lipid-phase transitions even though they have high water solubility. A phosphate-containing spin label demonstrated strong anisotropic motion in the lipid–water system above the phase transition but not below. The addition of cholesterol to the DML–water system removed the anisotropic motion of 2,2,6,6-tetramethyl-4-phosphopiperidine-*N*-oxyl (Tempophosphate) and obscured the detection of bound, trapped, and free water. In addition to the charge–charge interactions between Tempophosphate and DML, two other spin labels were used both in the charged and uncharged states. 2,2,6,6-Tetramethyl-4-aminopiperidine-*N*-oxyl (Tempamine) in the charged state showed extremely strong anisotropic motion, presumably due to the interaction between the charged amine and the phosphate group of DML. When only partially charged, Tempamine showed much less anisotropic motion. PCA was analyzed at pH values where the carboxyl group was protonated and unprotonated. The resulting interaction was different at the two pH values. These water-soluble spin labels mimic ionic or nonionic solutes. Upon freezing, the spin labels are shown to be expelled from the ice regions into the remaining aqueous regions. The usefulness of this approach in studying solute behavior when freezing occurs and potential studies involving aqueous regions of cytoplasm are considered.

In recent years many studies have concentrated on the organization of, or the physical state of, the lipid and protein components of biological membranes. Many of these, especially spin-label studies, have largely been responsible for developing the concept of membrane fluidity. The water associated with the cell membrane and the physical state of the aqueous cytoplasm, in general, have received less attention. The water associated with the cell membrane is probably important in modulating or controlling membrane structure and function. It is also conceivable that modifications of the membrane-associated water by ions or drugs could result in modifications of the membrane structure (Chapman et al., 1974; Hill, 1974).

There have been many speculations about the structure of intracellular water (Ling and Ochsenfeld, 1973; Drost-Hansen, 1971; Cooke and Kuntz, 1974). Such structured water could be important in controlling the translational diffusion of ions and other solute molecules. The organization of water and the environment it provides for solute molecules at phospholipid and membrane interfaces are relevant to membrane functional parameters in general.

Previous studies have treated the bound water associated with lipid structure using the techniques of calorimetry and deuteron magnetic resonance (Tanner and Stejskal, 1968; Ladbrooke and Chapman, 1969; Oldfield et al., 1971; Salsbury et al., 1972; Finer and Darke, 1974). It was revealed that up to 10 mol of water can be added per mol of lecithin before freezing of the water occurs. This was interpreted in terms of a complex hydrate structure around the polar head group and is referred to as bound water (Ladbrooke et al., 1968).

The lipid system itself undergoes a number of changes as the water content is increased. The initial amounts of water cause marked changes in the molecular motion of the lipid chains and also of the polar group motion (Salsbury et al., 1972). The bound or hydrated water considerably affects the lipid organization. The lecithins form a lamellar phase consisting of a phospholipid bilayer separated by layers of water and have a maximum hydration of 16–18 water molecules per lecithin molecule. Above this amount of water, two aqueous phases are formed, a lamellar phase and free water (Finer and Darke, 1974).

Previous studies have revealed a variety of information about the role of water in lipid bilayers. In the present paper we examine water-soluble spin labels in hydrated DML[1] multilayers. A description of the physical properties of spin-label solutes in the water zones treated here is fundamental to the understanding of solute distribution and translocation in the aqueous zones near membrane surfaces. Cholesterol is added to the DML–water system in parallel studies. Cholesterol causes drastic modifications of the associated water. After the addi-

† From the Biochemistry and Biophysics Department, The Pennsylvania State University, University Park, Pennsylvania 16802. *Received July 6, 1976.* This work was supported by the United States Energy Research and Development Administration AT(11-1)-2223.

‡ Visiting distinguished professor. Present address: Chelsea College, University of London, London, England.

[1] Abbreviations used: A_N, isotropic nitrogen hyperfine coupling; DML, dimyristoyllecithin; g_N, isotropic g value; h_0, first derivative mid-field line height; h_1, first derivative low-field line height; h_{-1}, first derivative high-field line height; h_{-1P}, first derivative line height of the polar component of the high-field line (shown in Figure 6); h_{-1H}, first derivative line height of the apolar component of the high-field line (shown in Figure 6); PCA, 2,2,5,5-tetramethyl-3-carboxypyrrolidine-*N*-oxyl; R_3, an empirical motion parameter; τ_c, rotational correlation time; Tempamine, 2,2,6,6-tetramethyl-4-aminopiperidine-*N*-oxyl; Tempo, 2,2,6,6-tetramethylpiperidine-*N*-oxyl; Tempone, 2,2,6,6-tetramethylpiperidone-*N*-oxyl; Tempophosphate, 2,2,6,6-tetramethyl-4-phosphopiperidine-*N*-oxyl; W_0, first derivative mid-field line width; Tris, tris(hydroxymethyl)aminomethane.

tion of cholesterol, the discrete zones referred to as bound, trapped, and free water lose their identity. The degree of immobilization and general motional properties of the spin labels located in aqueous zones are drastically altered after the addition of cholesterol. A final important aspect of this study is the redistribution of spin-label solutes during the freezing of water in the free and trapped zones. This aspect of the present study is relevant to the field of cryobiology.

Materials and Methods

A Varian *X*-band electron paramagnetic resonance spectrometer equipped with a laboratory-constructed variable temperature unit allowing continuous monitoring of cavity temperature to an accuracy better than +1 °C was used.

Dimyristoyllecithin (DML) was purchased from Sigma Chemical Co. (St. Louis, Mo.). The spin labels 2,2,6,6-tetramethylpiperidone-*N*-oxyl (Tempone), 2,2,5,5-tetramethyl-3-carboxypyrrolidine-*N*-oxyl (PCA), and 2,2,6,6-tetramethyl-4-amino-piperidine-*N*-oxyl (Tempamine) have had their synthesis and purifications described (Rosantsev, 1970). The synthesis of 2,2,6,6-tetramethyl-4-phosphopiperidine-*N*-oxyl (Tempophosphate) was carried out by published methods (Baer and McArthur, 1944). Diphenyl phosphoryl chloride (Aldrich Chemical Co., Milwaukee, Wis.) was condensed with Tempol in dry pyridine. The reaction product was reacted with 6 M $Ba(OH)_2$ for 8 h. The final product was purified by column chromatography using 200-mesh silica gel with methanol–ethyl acetate–acetic acid (9:1:1) as moving phase. The structures of spin labels used in this study are shown in Figure 1.

Dimyristoyllecithin was dried to constant weight under vacuum over metallic sodium. Aqueous spin label was added to 50-mg samples of phospholipid and the samples were sealed. The sealed samples were heated over steam for 1 h with intermittent vortexing. Samples were then transferred to capillary tubes, sealed in glass, and were then ready for analysis by electron spin resonance.

One of the primary information sources from spin labels is the state of rotational motion sometimes quantified as rotational correlation time τ_c. The equation $\tau_c = 6.5 \times 10^{-10}$ s$\{W_0[(h_0/h_{-1})^{1/2} - 1]\}$ has been previously used (Keith et al., 1974) and for isotropic motion is generally considered to be valid in the fast motion range. This equation has its general justification from the work of Kivelson (1960) and uses the crystal parameters of Griffith et al. (1965) measured for di-*tert*-butyl nitroxide and assumes a magnetic field setting of 3400 G. The exact crystal parameters giving rise to the constant, 6.5×10^{-10} s, will change slightly for different nitroxides. Different spin labels often have a very different minimum line width, limited by interactions with protons on the nitroxide structure. This may change the absolute values of τ_c for nitroxides of the same size. The exact nitroxide structure and functional groups also will modify τ_c values of a particular nitroxide in a given solvent. We use the τ_c equation given above in the analysis of Tempone motion. The other spin labels used for motional studies are treated in a more empirical manner. The constant, 6.5×10^{-10} s, is set equal to one and the resultant value, R_i, is treated as an empirical motion parameter, $R_i = W_0[(h_0/h_{-1})^{1/2} - 1]$, valid for purposes of comparative measurements. W_0 is the first derivative mid-line width, h_0 is the first derivative mid-field line height, and h_{-1} is the first derivative high-field line height.

Measurements made in regard to partitioning of Tempone, h_{-1H}/h_{-1P}, are shown in the lower right of Figure 2.

The anisotropic motion parameter, h_1/h_0, given in the analysis of Tempophosphate has a straightforward origin. Three separate reports (Nordio, 1970; Williams et al., 1971; Vasserman et al., 1971) have shown that anisotropic motion at *X* band about the nitroxide's *x*-principal axis in the fast tumbling range gives rise to a low-field line, h_1, of greater amplitude than the mid-field line, h_0. Isotropic motion at *X* band always has $h_0 \geq h_1$. It is possible that certain types of environmental heterogeneity may also give rise to this general type of signal.

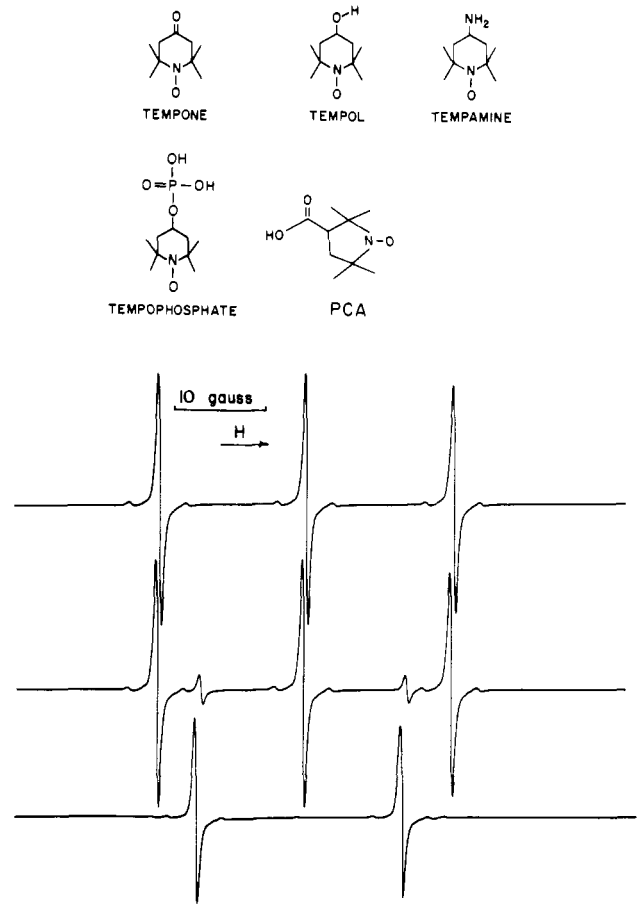

FIGURE 1: Structures of spin labels used. The chemical name for each spin label is given in the abbreviations and synthesis or references relating to the synthesis are presented in the Materials and Methods. The three spin labels containing pH-dependent ionizable groups are shown in the uncharged state. Comparative spectra for [^{14}N]Tempone and [^{15}N]Tempone. The top signal is taken from a 10^{-3} M solution of [^{14}N]Tempone. The second signal is taken from an aqueous solution of 10^{-3} M [^{14}N]Tempone which had a very fine capillary containing [^{15}N]Tempone inserted into it. The smaller [^{15}N]Tempone hyperfine lines can be readily seen. The third spectrum from the top is that of 10^{-3} s M [^{15}N]Tempone.

Isotropic hyperfine coupling (A_N) is the spacing in gauss between hyperfine lines. The isotropic *g* value determined from the midpoint of the integrated signal is given by $g = h\nu/\beta H$, Where *h* is Planck's constant, ν is the klystron frequency, β is the Bohr magneton, and *H* is the applied external magnetic field. Figure 2 shows spectra of [^{14}N]Tempone and [^{15}N]Tempone in water. [^{15}N]Tempone is an ideal standard for measuring hyperfine coupling constants and *g* values and was used for this purpose in these studies.

Results

The Detection of Different Physical States of Water. Tempone has solubility in liquid hydrocarbons and in water; therefore, in hydrocarbon–water systems, Tempone partitions

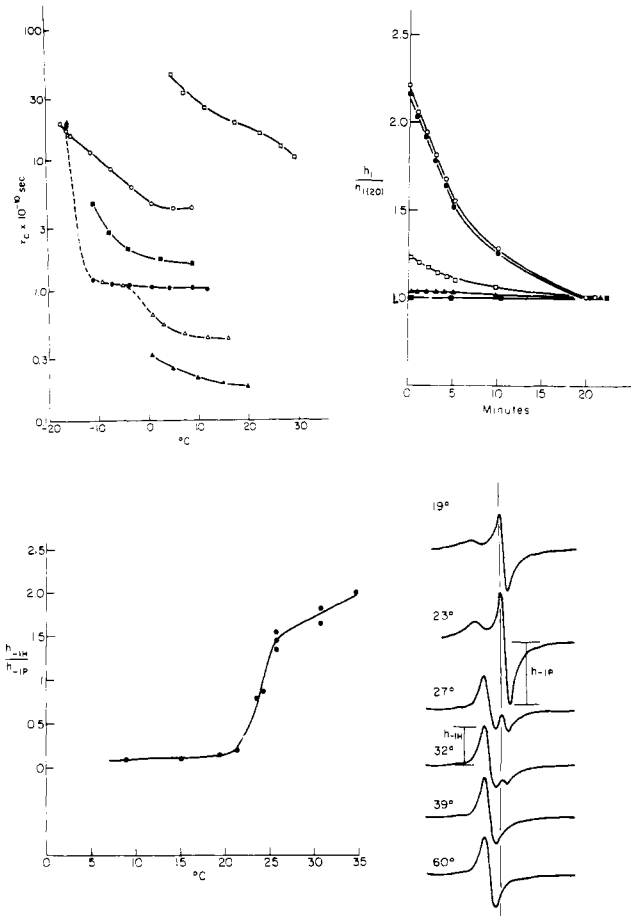

FIGURE 2: (Upper left) τ_c values of Tempone in DML–water systems. Each of the lines is described in the text and the appropriate notations are included here. (▲) Water alone; (△) 40 water per DML; (●) 20 water per DML; (○) 10 water per DML; (■) 40 water per DML plus cholesterol; (□) 20 water per DML plus cholesterol. The two samples with cholesterol contain cholesterol and DML in a mole ratio of 1. (Upper right) Hysteresis of the Tempone low-field line at −16 °C. (○) Forty water per DML; (●) 20 water per DML; (▲) 10 water per DML; (□) 40 water per DML plus cholesterol; (■) 20 water per DML plus cholesterol. Signal height measurements started at 90 s after cooling of the sample had been started. Each sample was cooled for 60 s in a liquid heat exchanger held at −16 °C and was then transferred to the spectrometer cavity which was also held at −16 °C. The low-field line height at the end of 90 s after the initiation of cooling is the first time point. The denominator shown on the ordinate is the line height of each sample after 20 min of exposure to −16 °C in the spectrometer cavity. (Lower left) Ratio of the high-field line components of Tempone in the DML–20 water sample as a function of temperature. (Lower right) The Tempone high-field line at various temperatures. The dramatic change in the ratio of the high-field line components as a function of temperature for the DML–20 water sample.

between the two phases. Using methyl myristate and water, Tempone favors the methyl myristate phase at room temperature by a factor of 1.7. Tempone added to the DML preparations results in a signal with the high-amplitude component originating from hydrocarbon zones above about 23 °C and primarily from aqueous zones below this temperature.

The motional state of Tempone is strongly influenced by the number of water molecules per DML molecule. Data obtained using Tempone as a spin label are shown in the upper left of Figure 2. The preparation containing 40 water molecules per DML molecule shows an increase in the τ_c of Tempone by about a factor of 2 compared with Tempone in water alone. The sample containing 20 molecules of water per DML has a further reduced motional freedom of Tempone. The lipid–water system containing 10 molecules of water per DML molecule results in the rotational motion of Tempone being still further reduced, to the extent of being about 40 times more immobilized than in free water.

The preparations containing 10, 20, and 40 water molecules per DML were analyzed for hysteresis effects at −16 °C (upper right of Figure 2). Each preparation was cooled from a starting temperature of 50 °C to a final temperature of −16 °C in an alcohol bath. A thermocouple inserted into the sample revealed that less than 1 min was required to reach temperature equilibrium. One minute was used for cooling. The samples were transferred rapidly to the instrument cavity and 30 s was given for instrument adjustments. Beginning at this time, the low-field line height was monitored as a function of time. The precooled cavity was maintained at −16 °C throughout the experiments. Figure 2 shows the time dependence of this line height change for the first 20 min.

Tempone dissolved in water alone results in rapid, approximately isotropic motion. The measured τ_c values of Tempone in water are shown in Figure 2. In water alone, there is some decrease in the rotational motion upon cooling in the temperature range 20 to 0 °C. Below 0 °C and after ice formation, most of the isotropic three-lined signal changes to an exchange narrowed signal. This signal has an expanded central line with greatly reduced low- and high-field lines. The general phenomenon of triplet signals from some spin labels being modified to exchange-narrowed singlets as a consequence of a pure liquid matrix going to the solid state has been previously described (Cohn et al., 1974). The present results are explained in a similar manner. As the ice crystal lattice forms in a matrix containing only spin label and water, the spin-label molecules apparently coalesce into zones of high spin-label concentration. This results in exchange narrowing of the spin-label signal.

Neither of the DML–water samples resulted in an exchange narrowed signal below 0 °C. The 40 water molecules per DML molecule sample did, however, result in a Tempone signal showing marked increase in restriction to rotational motion compared with just above 0 °C (see legend of Figure 2). There was no detectable exchange narrowed contribution in the signals at −5 or −10 °C. The integrated signal intensities of the low- and mid-field lines were the same above and below 0 °C (accuracy limits were estimated at ±10%). These data indicate that, as the free water freezes, the Tempone molecules become localized in the trapped and bound water zones.

As previously reported using differential scanning calorimetry, the trapped water in the bilayer undergoes supercooling and then freezes (Ladbrooke and Chapman, 1969). Apparently the time-dependent line height decrease of the Tempone signal at −16 °C reflects this freezing process. It appears that all the Tempone signal remaining after the trapped water freezes originates from the bound water region. The freezing process apparently occurs in two steps for the sample containing 40 water molecules per DML. One freeze occurs between 0 and −5 °C. The second freezing process occurs over a longer time. We monitored the second freezing process at −16 °C. At this temperature the 40 water and 20 water per DML samples demonstrated almost identical hysteresis. The second freezing process will occur, however, at temperatures above and below −16 °C. At the lower temperatures the process is faster and at the higher temperatures the process requires longer periods. No systematic measurements were carried out on the samples at other temperatures.

The sample containing 10 water molecules per DML showed no such effects as those demonstrated by the 40 water and 20 water per DML samples. The 10 water per DML sample resulted in gradual loss of the rotational motion of Tempone. The

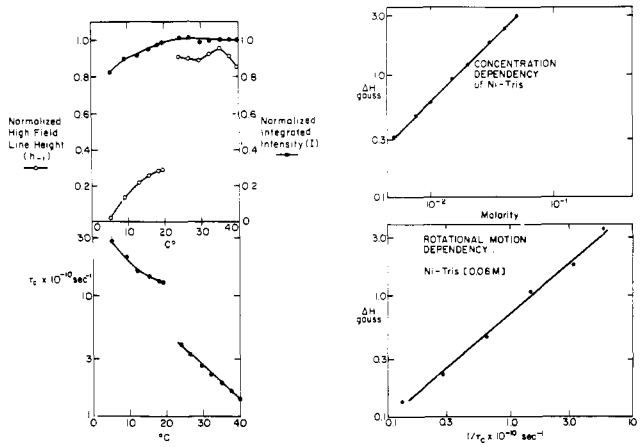

FIGURE 3: Data from the Tempone–DML–20 water sample containing 0.5 M nickel-Tris. The two graphs on the left show how the low-field line height, the integrated intensity of the low-field line, and τ_c all change as a function of temperature when the Tempone signal is entirely localized within the hydrocarbon zone of DML. The upper graph on the right shows how the line broadening of Tempone in aqueous medium is dependent upon the concentration of nickel-Tris. The lower graph on the right shows how this line broadening is dependent upon the viscosity-limited motion of Tempone.

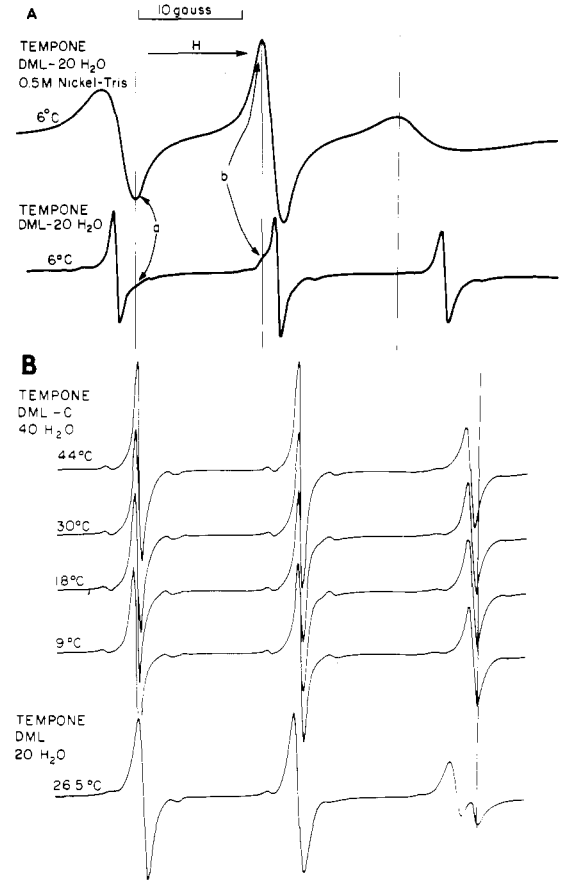

FIGURE 4: (A) Spectra of Tempone in the DML–20 water sample. The upper spectrum shows the residual signal of Tempone in the DML–20 water system after the aqueous signal has been removed by the interaction between nickel-Tris and Tempone. The lower signal shows that the aqueous line dominates in amplitude when no nickel-Tris is present. (a) Shows the residual low-field line component in the sample not treated with nickel-Tris which originated from Tempone dissolved in the hydrocarbon phase. (b) Shows the residual contribution of the mid-field line which originated from Tempone dissolved in the hydrocarbon phase. The instrument signal intensity was set 20 times higher for the signal which was taken in the presence of nickel-Tris and all other instrument settings were the same. The vertical lines show the relative spectral positions of the different contributions. (B) Comparative spectra of Tempone dissolved in DML ± cholesterol. The upper four signals comprising a temperature range contained 1 equiv of cholesterol. The lower signal does not contain cholesterol and was taken at a temperature where both hydrocarbon and aqueous components are clearly revealed in the high-field line. The upper four signals indicate the gradual change in the hyperfine coupling which occurs in the sample containing cholesterol. The upper four spectra are very nearly the same in terms of the measurements which are applicable to rotational motion equations.

final state of Tempone motion in the 10, 20, and 40 water samples at −16 °C is the same, indicating that Tempone experiences the same molecular environment in all three. The probable environment remaining at this temperature is bound water. There were no detectable exchange narrowed components in any of the samples at −16 °C.

The spectra of Tempone show resolution of polar (h_{-1P}) and nonpolar (h_{-1H}) contributions in the temperature range near 23 °C (lower left and right of Figure 2). The nonpolar contribution dominates above this temperature and the polar contribution dominates below this temperature. A plot of this line height ratio reveals the thermotropic phase transition between 20 and 25 °C. The line widths of the two contributions are approximately the same in this temperature range.

We use nickel-Tris as a paramagnetic broadening agent to selectively remove the Tempone aqueous signal. The chelate, nickel-Tris, has essentially no hydrocarbon solubility and broadens the Tempone hyperfine lines by an electron-spin exchange process. Nickel chelates have previously been used to broaden the hyperfine lines of nitroxides (Anisimov et al., 1971).

Figure 3 shows the concentration dependency of nickel-Tris for the broadening of the Tempone low-field line. Figure 3 also shows the motional dependency for broadening of the Tempone low-field line by nickel-Tris. The remaining spectra of Tempone appear considerably different after removal of the polar contributions. Without nickel-Tris, the polar component dominates at temperatures below about 23 °C. Figure 3 shows a plot of τ_c vs. temperature taken from spectra which have the polar components removed. A pronounced reduction in motion occurs in the vicinity of 23 °C. Figure 4 shows comparative spectra plus and minus 0.5 M nickel-Tris. This figure reveals traces of the hydrocarbon signal in the sample not treated with nickel-Tris. Because of the strong effect of molecular motion on collisional dependent line broadening, 0.5 M nickel-Tris was required to remove the aqueous signal. Under conditions where greater freedom of molecular motion of the spin label is allowed, much less nickel-Tris is sufficient to remove the aqueous signal (upper right, Figure 3).

Figure 3 also shows the high-field line height over the same temperature range. There is a drastic change in line height. Partitioning between the hydrocarbon and aqueous phases, however, is determined by measuring the integrated intensity of one of the ^{14}N-hyperfine lines. For present purposes, the low-field hyperfine line was selected. The line height changes drastically because the area under a first derivative Lorentzian line is proportional to W^2h.

The Effect of Cholesterol on the Motion of Tempone. The addition of equimolar cholesterol to DML in the samples containing 20 or 40 water molecules per DML caused further immobilization of Tempone. The data presented in Figure 2 show that hysteresis effects, apparently caused by freezing of trapped water, do not occur at the same temperature after the addition of cholesterol. The general state of rotational motion is drastically modified in both samples containing cholesterol. Figure 2 indicates that cholesterol added to the 40 water

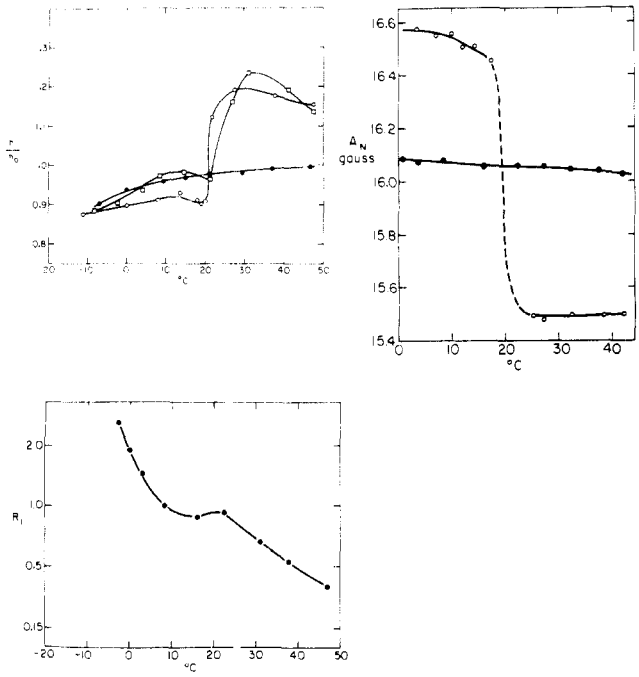

FIGURE 5: Motional properties of Tempophosphate dissolved in DML. (Upper left) The anisotropic motion parameter, h_1/h_0, is shown with the DML at two different hydration states and in the presence of cholesterol. The pH was maintained at 7.0 for all three analyses. (○) Twenty water per DML sample; (●) 20 water per DML plus 1 molecular equiv of cholesterol; (□) 10 water per DML sample. (Upper right) (○) Twenty water per DML sample; (●) 20 water per DML plus cholesterol. Hyperfine coupling is shown as a function of temperature in the two samples. (Lower left) The empirical motion parameter, R_i, is shown as a function of temperature in the 20 water per DML plus cholesterol sample.

molecules per DML sample removes a free water component. This extra water must now be accommodated in the lamellar structure of the DML. Cholesterol increases the spacing between adjacent phosphorylcholine groups due to the intercalation of cholesterol molecules. This increased spacing must have a profound effect on the physical state of interfacial water. Solute molecules such as Tempone experience this modified environment and in turn have their motional properties modified. The addition of cholesterol takes away the properties which make the inference of bound, trapped, and free water as discrete entities possible, at least for the concentrations we used.

Figure 4A shows comparative spectra for the 40 water per DML sample. In the range from 44 to 9 °C, the sample containing cholesterol shows no evidence of Tempone occupying two distinct environments. Instead, there is a slight, gradual increase in A_N with decreasing temperature. The Tempone signal from the DML–cholesterol sample shown in Figure 4B illustrates the high-field line positions in a sample that does show partitioning between aqueous and hydrocarbon zones.

Motion of Tempophosphate in DML Multilayers. Tempophosphate dissolved in the 10 or 20 water molecules per DML sample results in a highly anisotropic signal above 23 °C (Figure 5). The motion below 23 °C is comparatively isotropic. The detection of pronounced anisotropic motion about the x principal axis of the spin label at X band is detected by measurements of the line height ratio, h_1/h_0. Enhanced motion about the x principal axis of a nitroxide molecule has been treated previously in at least three independent reports (Nordio, 1970; Vasserman et al., 1971; Williams et al., 1971).

As the line height ratio, h_1/h_0, increases in response to temperature elevation, the A_N concomitantly decreases. At temperatures below 23 °C the ratio, h_1/h_0, is less than one and the A_N is more characteristic of an aqueous environment. These data are consistent with the analysis that the phosphate group of Tempophosphate interacts with the positively charged choline groups at the bilayer interface. At temperatures below 23 °C the piperidine ring is more localized in the interlamellar water. As the temperature is elevated above 23 °C, the polar groups undergo some separation and the DML lattice expands allowing the piperidine ring to orient toward the bilayer hydrocarbon zone. This position would be expected to result in enhanced motion about the x principal axis of the nitroxide and probably also to lower the A_N. The anisotropic motion parameter, h_1/h_0, gives no indication of a phase transition between −10 and 50 °C for the sample containing 20 molecules of water per DML plus cholesterol (Figure 5). However, when the data are plotted differently as shown in the lower left of Figure 5, then it is possible to infer a nonlinear event in the neighborhood of 10–20 °C. This empirical motion parameter, R_i, indicates sensitivity to an event which is not apparently observed in the partitioning of Tempone or the anisotropic motion of Tempophosphate.

Measurements of the A_N of Tempophosphate were taken for the 20 water per DML sample and the sample containing cholesterol. Figure 5 (upper right) shows a dramatic change in A_N between 25 and 17 °C. The A_N of the Tempol molecule in hexane and other alkanes is 15.2 G. The A_N of Tempophosphate never drops to a comparable value. The nitroxyl group of Tempophosphate probably never extends completely into a water-free hydrocarbon zone. The A_N of Tempophosphate in bulk phase water is 17.1 G, indicating that the interfacial location of Tempophosphate does not have the same properties as it does in the bulk phase water.

The Molecular Motion of Tempamine Dissolved in Multilayers of DML. Tempamine was analyzed in 20 water molecules per DML under two ionic conditions. Figure 6 shows the ratio, h_1/h_0, plotted as a function of temperature. In one case, the pH of the aqueous phase was maintained at 6.0 to ensure complete ionization of the amine group (closed squares, Figure 6). Under these conditions the Tempamine molecule undergoes extremely anisotropic motion about the x principal axis. The resulting charge–charge interaction is apparently between the charged amine of Tempamine and the charged phosphate group of DML. Figure 6 shows that the hyperfine coupling constant, A_N, maintained a constant value throughout the entire temperature range. This A_N value of 16.8 for tempamine indicates a polar environment near that of water. Figure 6 also shows the parameter, h_1/h_0, plotted against temperature, while the aqueous phase is maintained at a pH of 10.0. The pK_a of Tempamine is near 9.5; therefore, elevating the pH to 10.0 does not completely neutralize the Tempamine molecule. Figure 6 shows how the A_N of Tempamine undergoes considerable change at the different temperatures shown when the pH is maintained at 10.0. The amine group at a pH of 10.0, however, must still have a strong interaction with the phospholipids, as is evidenced by the anisotropic motion revealed in Figure 6. The spectra shown in Figure 6 allow direct comparisons of the degree of anisotropic motion as is indicated by the low- and mid-field line amplitudes at these two pH values.

Figure 6 also shows the anisotropic motion parameter, h_1/h_0, of Tempamine dissolved in a sample of DML containing 1 mol equiv of cholesterol and 20 water molecules per DML. The pH was maintained at 6.0 where Tempamine should be in the fully charged state. The degree of anisotropic motion is drastically reduced as is indicated by the plot of h_1/h_0 against temperature

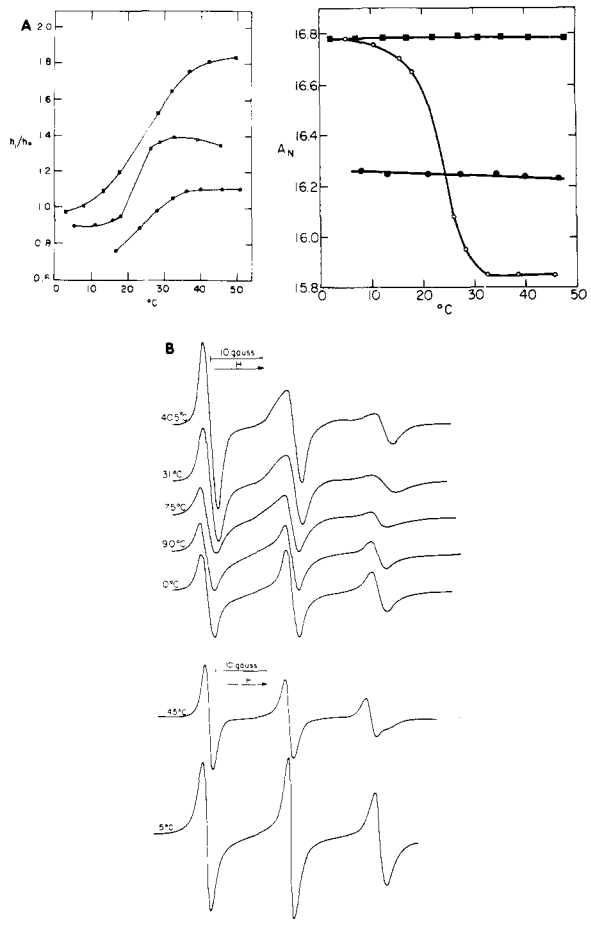

FIGURE 6: (A) (Left) Motional properties of Tempamine dissolved in DML. Anisotropic motion of Tempamine. (■) Tempamine dissolved in 20 water molecules per DML at a pH of 6.0; (○) 20 water per DML sample at a pH of 10.0; (●) 20 water per DML plus cholesterol sample maintained at a pH of 6.0. (Right) Hyperfine coupling constant of Tempamine in DML samples. (■) Twenty water molecules per DML at a pH of 6.0; (○) 20 water molecules per DML at a pH of 10.0; (●) 20 water molecules per DML plus cholesterol at a pH of 6.0. (B) Spectra of Tempamine in DML. The top five spectra were taken from the 20 water per DML sample at pH of 6.0. The bottom two spectra were taken from the 20 water per DML sample at a pH of 10.0.

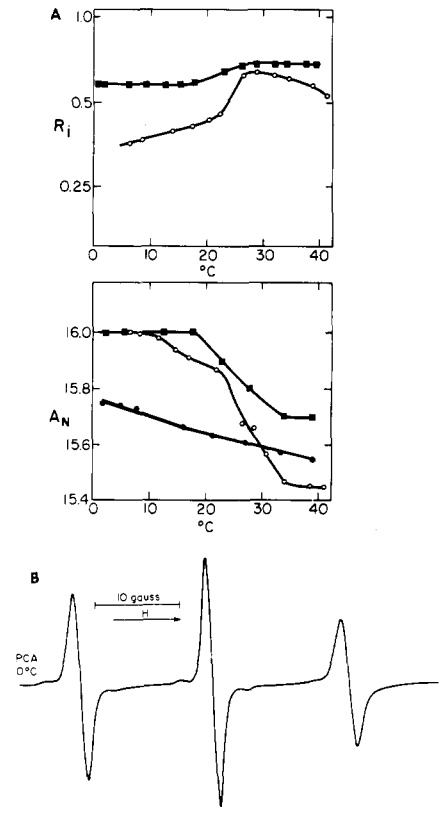

FIGURE 7: (A) Motional properties of PCA dissolved in DML. The upper plot shows R_i values of the 20 water molecules per DML sample at a pH of 8.0 (■) and at a pH of 3.0 (○). The lower plot shows the hyperfine coupling of PCA dissolved in the 20 water molecules per DML at a pH of 8.0 (■), at a pH of 3.0 (○), and at a pH of 8.0 with 1 equiv of cholesterol (●). (B) Spectrum of DML dissolved in the 20 water per DML at 2 °C.

shown in Figure 6. The A_N stays at a constant value for the measurable temperature range, 10 to 50 °C. The A_N is very close to 16.2 for this entire range, indicating a local environment having a polarity between that of an aqueous and a hydrophobic environment. The constancy of the A_N over this temperature range in the cholesterol-containing sample indicates that the local environment seen by the Tempamine molecule has the same polarity throughout this temperature range.

The Molecular Motion of PCA Dissolved in Multilayers of DML. The spin label PCA is unlike either of the other three used in that it is a pyrrolidine while the others are piperidines. The two charged piperidines have a plane of symmetry perpendicular to the nitroxide y axis, passing through both the nitroxyl group, and the charged group at ring position four. Anchoring the charged group by a charge–charge interaction in a confined space will result in molecular rotation about an axis that is nearly parallel to the nitroxide x axis. PCA, on the other hand, is a five-membered ring with a carboxyl group attached to carbon three of the pyrrolidine ring. A strong ionic interaction between this carboxyl group and the positively charged choline groups of DML will not cause PCA to preferentially rotate on either the x, y, or z principal axes of symmetry. Instead, the axis of rotation is diagonal to all three. This does not result in any readily recognizable type of anisotropic spectrum. Anisotropic rotation about axes diagonal to the principal axes of symmetry have been treated by computer simulation (Vasserman et al., 1971).

Spectra of PCA were also taken at two different pH values. Figure 7A shows how the empirical motion parameter, R_i, varies with temperature with PCA in the ionized state at a pH of 8.0 (closed squares) and in an un-ionized state at a pH of 3.0 (open circles). The degree of motional freedom is greater at all temperatures for un-ionized PCA. Figure 7A shows that the A_N values vary for both the charged and the uncharged states but that the variations are greater for the uncharged state. Uncharged PCA, having less polar interaction than charged PCA, is probably more susceptible to changes in the physical state of the hydrocarbon zones of DML. Even in the ionized state, the charge–charge interactions are not of sufficient strength to keep the nitroxyl group in a constant environment. Figure 7B shows a representative spectrum at a pH of 8.0 in the 20 water molecules per DML molecule sample. Spectra of PCA in DML all have the same general appearance.

The addition of cholesterol to the 20 water DML sample caused a drastic increase in the R_i values. The R_i values ranged between 1.5 and 3.0 and are off the scale shown in Figure 7. The addition of cholesterol decreased the A_N in an analogous way to that of Tempamine in the comparable sample (closed circles of Figure 7B).

Discussion

Effects Associated with the Phospholipid Thermotropic Phase Transition. It is now well known that important changes occur in lipids above the phase transition temperature, e.g., the lattice expands, the chains melt and have some rotational isomerization, the polar groups become more mobile, and the lamellae decrease in width (Ladbrooke et al., 1968). Phase transition or phase separation events have been examined by a variety of methods including x-ray diffraction, nuclear magnetic, and electron spin resonance spectroscopy. Spin labels which have been used to study lipid phase change events localize in the hydrocarbon chain region or partition between the hydrocarbon phase and the aqueous phase. A small spin label, Tempo, which favorably partitions into hydrocarbon zones has been used in cases where the volume of the aqueous zone predominates. This probe has been used to detect phase separations in lipid and membrane systems (Shimshick et al., 1973). The aqueous signal of Tempo, in these studies, was predominantly from bulk water. The information about the systems was obtained by observing the relative hydrocarbon and aqueous line height contributions resulting from Tempo partitioning between the two environments of the aqueous membrane sample being analyzed. In the present study Tempone is used in much the same way for the detection of change in the physical state of the lipid zones, except the aqueous phase is a much smaller proportion of the total system. Reducing the comparative volume of the aqueous phase and using a spin label such as Tempone which has higher water solubility than that of Tempo acts somewhat in a compensating way. Under these conditions, Tempone is localized in the hydrocarbon zones to a considerable degree as is clearly indicated in Figure 2. A surprising aspect of this partitioning, however, is the observation that the actual partition coefficient may not undergo much of a change at the phase transition temperature. The use of the chelate, nickel-Tris, effectively removed all of the component arising from Tempone dissolved in the aqueous phase and, therefore, made possible measurements quantifying the Tempone signal originating from the hydrocarbon zone, over a large temperature range. These data, shown in Figure 3, indicate that the DML multilayers must be taken to a temperature considerably below that of the observed phase transition before very much of the Tempone dissolved in the hydrocarbon phase is actually "pushed" out into the aqueous phase. The apparent change in partitioning, as measured by line-height ratios, appears to be entirely due to a change in the motional state of Tempone in the hydrocarbon phase. The change in motional state drastically reduces the high-field hydrocarbon line height contribution.

It is of interest to note that, even in the preparations used here where the spin labels have high water solubility, the detection of phase transition behavior still appears to originate from an interaction between the spin label and the hydrocarbon phase of the membrane. In the case of Tempone, it is due to a drastic change in the motional state at 23 °C and below. In the case of Tempophosphate it is due to a change in anisotropic motion and to a change in the localization of the *N*-oxyl group. Tempamine in the charged state maintains a constant hyperfine coupling (A_N) value in the multilayers but undergoes a drastic change in anisotropic motion over the temperature range shown in Figure 6. Tempamine at a pH of 6.0 does not reveal any drastic change at 23 °C. Instead, the change in anisotropic motion is continuous and gradual over the entire temperature range from several degrees below 23 °C to several degrees above 23 °C. It is only when the pH of Tempamine is modified to that of the uncharged state, where it is dissolved in the hydrocarbon phase to a considerable extent, that it reveals a phase transition. The spin label containing the carboxyl group, PCA, behaves in an analogous fashion to Tempamine. In the charged state, as is revealed in Figure 7, the rotational motion undergoes only a slight change over a large temperature range. Maintaining the pH at 3.0 where PCA is uncharged reveals information about the phase transition event, as is shown in Figure 7. There the rotational motion undergoes a fairly drastic change between about 20 and 23 °C. The change in hyperfine coupling that occurs with PCA in the charged state indicates that its charge–charge interaction is of a smaller magnitude than that of Tempamine or Tempophosphate. The charged carboxyl group of PCA must have a more diffuse charge localization than either of the other two charged groups used. It appears that this diffuse charge localization results in less interaction between the charged carboxyl group of PCA and the charged choline groups of DML than occurs with the charged phosphate group of Tempophosphate. The A_N of PCA undergoes some detectable change even when it is maintained in the charged state. Maintaining PCA at a lower pH where it is uncharged considerably amplifies the degree to which the hyperfine coupling is modified.

All of these data collectively indicate that even in the DML multilayer system and using spin labels that have high water solubility, the detection of a phase transition event is still primarily based on the interaction between the spin label and the hydrocarbon phase. The physical events leading to a thermotropic phase transition must be complex. The expansion of the hexagonal lattice sites probably results in increased hydration shells around both phosphate and choline groups. The increased hydration shells must result in modification of the physical state of the interlamellar water. Although, in the present experiments, we detect the thermotropic phase transitions by observation of events which we normally associate with the lipid phase, the physical modifications must involve both lipid and water zones.

The Effect of Cholesterol on Interfacial Water. The addition of equimolar cholesterol to DML in the samples containing 20 or 40 water molecules per DML caused further immobilization of Tempone. Previous spin-label studies have analyzed the effect of cholesterol on the hydrocarbon portion of phospholipids. These studies revealed that the addition of cholesterol resulted in fatty-acid-bearing and sterol-bearing spin labels being more restricted in regard to rotational diffusion (Smith, 1972; Lapper et al., 1972). Sterol and fatty acid spin labels also displayed a greater degree of orientation in oriented multiyers containing cholesterol. Our studies indicate that the aqueous interface is also modified by cholesterol. The data presented in Figure 2 show that hysteresis effects, apparently caused by freezing of trapped water, do not occur at the same temperature after the addition of cholesterol. The general state of rotational motion of Tempone is drastically modified in both samples containing cholesterol. Cholesterol increases the spacing between adjacent phosphorylcholine groups due to the interaction of cholesterol molecules. This increased spacing must have a profound effect on the physical state of interfacial water. The partitioning of Tempone was modified to the extent that only a homogeneous appearing signal can be seen after the addition of cholesterol. In fact, the addition of cholesterol takes away the properties which make the inference of bound, trapped, and free water as discrete aqueous zones possible, at least for the concentrations of materials that we used here.

The addition of cholesterol removed anisotropic motion from the Tempophosphate molecule and drastically reduced the anisotropic motion of Tempamine. Cholesterol added to the

DML preparations decreased the freedom of molecular motion of all four spin labels. The three spin labels which allowed A_N measurements throughout the temperature range resulted in nearly constant A_N values. In each case the A_N values decreased at lower temperatures and increased at higher temperatures compared with the same preparations not containing cholesterol. This indicates that cholesterol stabilizes the bilayer interface to changes that are normally associated with the thermotropic phase transition.

Dynamic Aspects of Spin-Label Solutes. Arguments are presented in the Results to show that when free, trapped and bound water are all present Tempone resides in all three. Upon freezing of the free water, the Tempone molecules residing in this zone move into the remaining liquid zones, trapped and bound water. We speculate that intracellular solutes, in general, may concentrate at membrane surfaces during the water-to-ice freezing process. The spatial distribution of solutes would be modified by freezing and cellular membranes would now be in an altered environment. Appropriate experiments using this general approach could well describe many of the events important to cryobiology.

Modification of charge on Tempamine and PCA modified both motional properties and spin-label localization in the multilayer system.

Tempophosphate was assayed only in the charged state; its A_N value changed from about 15.5 to about 16.6, from just above to just below the phase transition. Simultaneously, the anisotropic motion present at temperatures above about 23 °C was lost at lower temperatures. These two measurements, considered together, indicate that the phosphate group on Tempophosphate interacted with the DML–choline groups through a charge–charge interaction. This should result in the nitroxide ring structure being oriented in toward the bilayer hydrocarbon zone at temperatures above 23 °C. This position would be expected to result in anisotropic motion about the spin label x principal axis and to simultaneously reduce the A_N. At temperatures below the thermotropic phase transition where the alkyl chains of DML interact more strongly and pack tighter compared with temperatures above 23 °C, the nitroxide ring must be forced out into the aqueous phase of the multilayers. This would be expected to result in less anisotropic motion and an increased A_N. The expectations concerning the anisotropic motion parameter, h_1/h_0, and concerning the environmental polarity parameter, A_N, are consistent with the results.

Tempamine in the charged state exhibited more pronounced anisotropic motion than Tempophosphate even though they both have the same ring structure. The A_N values determined from spectra of Tempamine in DML were unchanged throughout the temperature range at a pH of 6, yet the parameter h_1/h_0 decreased as temperature decreased. Tempamine exhibited h_1/h_0 values considerably greater than one only when the A_N values were the highest observed. These two data indicate that the amine group of the spin label interacted with the phosphate group of DML and that the nitroxide ring was oriented out toward the aqueous layer. With uncharged Tempamine, as the A_N decreased, the apparent anisotropic motion was also lost.

The data regarding the dynamic properties of spin-label solutes all indicate that concomitant events occur in the lipid phase and the water phase. The modified interfacial properties of bilayers probably extended from the hydrocarbon phase to a significant depth into the interfacial water. This aqueous interfacial zone is probably very important to many processes associated with membrane functions.

References

Anisimov, O. A., Nikitaev, A. T., Zamaraev, K. I., and Molin, Yu. N. (1971), *Teor. Eksp. Khim. 7,* 682.

Baer, E., and McArthur, C. S. (1944), *J. Biol. Chem. 154,* 451.

Chapman, D. (1975), *Q. Rev. Biophys. 8,* 185.

Chapman, D., Urbina, J., and Keough, K. M. (1974), *J. Biol. Chem. 249,* 2512.

Cohn, G., Keith, A. D., and Snipes, W. (1974), *Biophys. J. 14,* 178.

Cooke, R., and Kuntz, I. D. (1974), *Annu. Rev. Biophys. Bioeng. 2,* 95.

Drost-Hansen, W. (1971), in Chemistry of the Cell Interface, Brown, H. D., Ed., New York, N.Y., Academic Press, p 58.

Eletr, S., Williams, M. A., Watkins, T., and Keith, A. D. (1974), *Biochim. Biophys. Acta 339,* 190.

Finer, E. G., and Darke, A. (1974), *Chem. Phys. Lipids 12,* 1.

Griffith, O. H., Cornell, D. W., and McConnell, H. M. (1965), *J. Chem. Phys. 43,* 2909.

Hill, M. W. (1974), *Biochim. Biophys. Acta 356,* 117.

Keith, A. D., Horvat, D., and Snipes, W. (1974), *Chem. Phys. Lipids 13,* 49.

Keith, A. D., Sharnoff, M., and Cohn, G. E. (1973), *Biochim. Biophys. Acta 300,* 379.

Keith, A. D., and Snipes, W. (1974), *Science 183,* 666.

Kivelson, D. (1960), *J. Chem. Phys. 33,* 1094.

Ladbrooke, B. D., and Chapman, D. (1969), *Chem. Phys. Lipids 3,* 304.

Ladbrooke, B. D., Williams, R. M., and Chapman, D. (1968), *Biochim. Biophys. Acta 150,* 333.

Lapper, R. D., Patterson, S. J., and Smith, I. C. P. (1972), *Can. J. Biochem. 50,* 969.

Ling, G. N., and Ochsenfeld, M. M. (1973), *Science 181,* 78.

McConnell, H. M., and McFarland, B. G. (1970), *Q. Rev. Biophys. 3,* 91.

Nordio, P. L. (1970), *Chem. Phys. Lett. 6,* 250.

Oldfield, E., Chapman, D., and Derbyshire, W. (1971), *FEBS Lett. 16(2),* 102.

Oldfield, E., Keough, K. M., and Chapman, D. (1972), *FEBS Lett. 23(3),* 285.

Rosantsev, E. G. (1970), Free Nitroxyl Radicals, New York, N.Y., Plenum Press, p 203.

Salsbury, N. J., Darke, A., and Chapman, D. (1972), *Chem. Phys. Lipids 8,* 142.

Shimshick, E. J., Kleeman, W., Hubbell, W. L., and McConnell, H. M. (1973), *J. Supramol. Struct. 4,* 285.

Smith, I. C. P. (1972), in Biological Applications of Electron Spin Resonance, Swartz, H. M., Bolton, J. R., and Borg, D. C., Ed., New York, N.Y., Wiley, pp 484–535.

Tanner, J., and Stejskal, E. (1968), *J. Chem. Phys. 49,* 1768.

Vasserman, S. M., Kuznetsov, A. N., Kovarskii, A. L., and Bychachenko, A. L. (1971), *A. Strukt. Khim. 12,* 609.

Williams, J. C., Mehlhorn, R., and Keith, A. D. (1971), *Chem. Phys. Lipids 7,* 207.